LRP 414/90 September 1990

Invited Paper presented by
M.Q. Tran at the
INTERNATIONAL WORKSHOP on
STRONG MICROWAVES IN PLASMAS

Suzdal, USSR, September 18-23, 1990

QUASI-OPTICAL GYROTRON DEVELOPMENT AT THE CRPP

The CRPP/ABB Quasi Optical Gyrotron Development Group
presented by M. Q. Tran
Centre de Recherches en Physique des Plasmas
Association Euratom-Confédération Suisse
Ecole Polytechnique Fédérale de Lausanne
21 Av. des Bains, 1007 Lausanne-Switzerland

Abstract - The operation of the 100GHz quasi-optical (Q.O.) gyrotron of the Centre de Recherches en Physique des Plasmas in Lausanne is described. Power up to 90kW and efficiency up to 12% have been achieved. Other features of the Q.O. gyrotron include single longitudinal mode operation, frequency tunability. Second harmonic emission (200GHz) has been observed with a resonator designed for operation at the fundamental. The issues pertinent to the Q.O. gyrotron concept are also discussed.

I) Introduction

The use of electron cyclotron waves (ECW) in fusion plasmas requires CW sources in the frequency range of 100-300GHz at power level of 0.5MW to 1MW per tube. The gyrotron is presently the most developed source for such applications. Two gyrotron concepts are presently under study, differing mainly in the resonant structure in which the interaction between the electromagnetic (EM) wave and the electron beam occurs. In the conventional gyrotron, the resonant structure is a cylindrical cavity operating in the TE^{o}_{mn1} mode. As an alternative to this concept, the quasi-optical (Q.O.) gyrotron was proposed, where the resonant structure is a Fabry-Pérot resonator placed transversely to the electron beam and operating in the gaussian TEM_{00q} mode. The advantages of the Q.O. concept are the frequency tunability and the geometric separation between the spent electron beam and the microwave output. The former characteristic offers flexibility for experiments on fusion devices, where it may be advantageous to change the localization of the power deposition zone without having to modify the magnetic field and therefore affecting the plasma properties.

The latter feature facilitates the design and the implementation of high power collector or depressed collector.

The theory of the Q.O. gyrotron was first presented in the late sixties by Rapoport et al. and other Russian physicists [1]. Further theoretical development can be found in several more recent references [2,3,4]. Experimental investigations were performed with a Fabry-Pérot resonator placed parallel [5] and perpendicular [6,7,8,9] to the electron beam. In this paper, we shall review some of the works being performed at the Centre de Recherches en Physique des Plasmas (CRPP) in the field of Q.O gyrotron and discuss some of the issues for future development.

II) Experimental set-up

The experimental set-up at the CRPP is described in figure 1. The magnetic field is created by a large superconducting coil system with a room temperature bore of 40cm and an axial gap of 15cm. In the cathode region, two gun coils were used to adjust the field and its gradient at the cathode surface. A magnetic field $\underline{B}_o$ up to 4T could be generated in the interaction region and a compression ratio of 20 is achieved between the cathode and the interaction zone. The operating

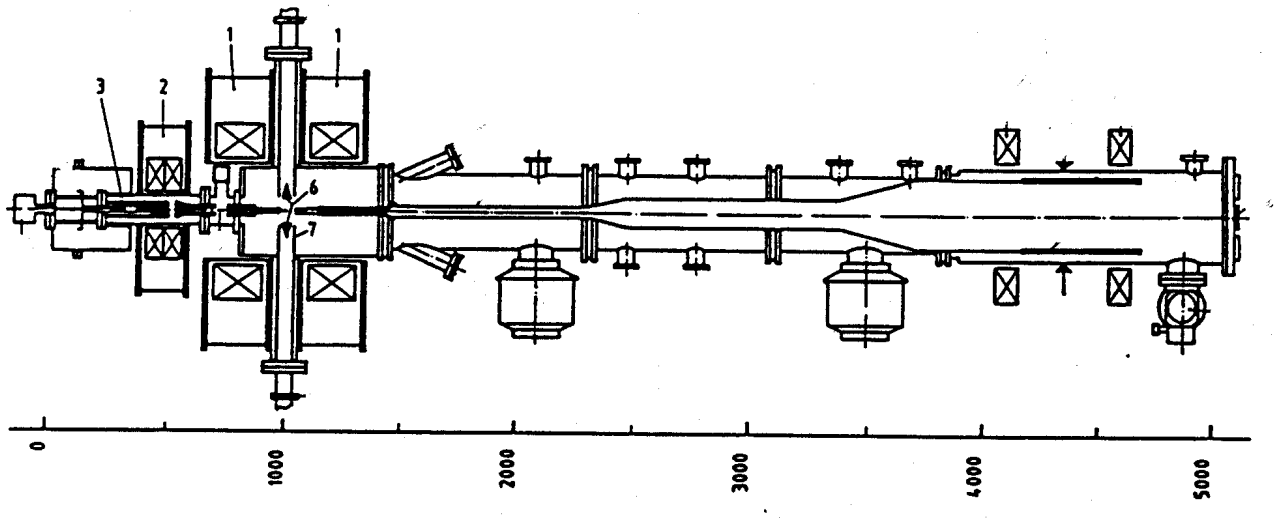

Figure 1.
Experimental set up. The main components are the main coils (1), the gun coils (2), the electron gun (3) and the mirrors (6,7) inside the vaccum vessel.

frequency was 100GHz for the fundamental frequency $\omega \sim \Omega/\gamma$ where Ω and γ are the non relativistic cyclotron frequency and the relativistic factor.

The electron beam was created using a standard Magnetron Injection Gun (MIG) which delivered an annular electron beam. The gun was originally designed for operation at 120GHz, but, due to operational constraints of the magnet, had to be adapted for operation around 100GHz. From the Hermannsfeldt EGUN code, the designed value of the ratio $\alpha=v_\perp/v_\parallel$ was 1.49 with a spread $\Delta\alpha/\alpha$ of 21%. However during the optimization of the output power, the current in the gun coils had to be set to values different from the designed ones, resulting in a lower value for α (α =1.12). The electron beam was guided by a beam tunnel (diameter =1cm) along its entire trajectory, except over 12cm (equivalent to 8 spot sizes w_o) in the interaction region.

The resonator was formed by two spherical mirrors made out of gold-plated copper. Since the experiment was pulsed at low duty cycle (pulse length = 15ms with a maximum repetition rate of approximately one shot per 30s), no cooling was necessary. Experiments were performed with and without a cylinder (diameter =15cm) enclosing the whole resonator up to the output waveguide. This cylinder is similar to the magnet cross bore of the compact version [7,8] of a Q.O. gyrotron. It did not influence the performances of the device.

The power was coupled out through an annular slot cut in each mirror. The slot width was 16.5mm and its inner edge was located at r = 28.5mm as measured from the resonator axis. The output transmission T and the coupling efficiency (i.e. the fraction of the diffracted energy which passed through the slot compared to the total diffracted power) were computed using a numerical code [10] based on Kirchoff's formulation of the Huyghens-Fresnel principle. For the TEM_{00q} gaussian mode, the power transmission of the resonator was about 4% with a coupling efficiency of 90%. Transverse modes TEM_{mnq} (m = radial index $\neq$ 0, n = azimuthal index $\neq$ 0) had a larger output transmission and could not be excited. The parameters of the experiments are summarized in Table I.

The microwave output power was extracted from both mirrors and guided through two, smooth-wall, overmoded waveguides (diameter 86.9mm). Since the resonator was symmetric, an equal amount of power

was extracted from both mirrors. The vacuum windows were Kapton foils of 125μm over the waveguide diameter. These windows could withstand power densities up to 1.5kW/cm^2 during the 15ms pulses. The same windows have been used for the last one and a half year.

Gyrotron frequency [GHz]	100
Electron beam	
Gun structure	Triode
Beam voltage V_b[kV]	65-70
Mod-anode votage V_a[kV]	25-30
Current I[A]	≤12
Compression ratio	20
Designed $\alpha = v_\perp/v_{\|\|}$	1.49
Optimum value of α	1.12
Beam radius r_b [mm]	2.13
Pulse length [ms]	15
Resonator characteristics	
Mirror radius of curvature R [cm]	50
Mirror separation d[cm]	34
g= 1-d/R	+0.32
Beam waist w_o[cm]	1.51
kw_O at 100GHz	31.7
Inner diameter of slot $\emptyset_i$[mm]	57
Fresnel number correponding to $\emptyset_i$	0.8
Outer diameter of slot [mm]	90
Outer diameter of mirror [mm]	136
Longitudinal mode separation [MHz]	440
Output transmission T[%] @ 100GHz, TEM_{00q}	4
Diffractive Q @ 100GHz, TEM_{00q}	34900
Ohmic/Diffractive loss [%]	5
Total Q @ 100GHz, TEM_{00q}	33200
Total Q @ 200GHz, TEM_{00q}	880000
Total Q @ 200GHz, TEM_{01q}	460000

Table I - Parameters of the Q.O. gyrotron

For power measurements, two different calorimeters were used. An electronic Scientech laser calorimeter was modified for optimum absorption in the 100GHz range by coating its surface with 3M Nextel® paint. This coating had to be periodically replaced since the microwave pulses burned the absorbing layer. A second calorimeter using Octanol $C_8H_{18}O$ as the absorbing medium was also built [11]. Octanol was selected for its RF dielectric properties [12] and its high boiling point (195°C). The measured reflection coefficient of the Octanol calorimeter was less than 5%. To measure the power of spurious second harmonic emission (Frequency = 200GHz), the technique used by Byerly et al. [13] was implemented. For this purpose, absorber plates (Macor) which had different absorption coefficients at 100GHz (k_i = 0.75 Np/cm) and 200GHz (k_i = 2.0 Np/cm) [14] were inserted into the microwave beam. Each absorber plate thickness was selected to be $n\lambda_{mat}/2$, where λ_{mat} is the wavelength in the absorber at 100GHz. We thus minimized effects due to reflection at the fundamental and the second harmonic. With increasing thickness (by stacking the plates), the content of the second harmonic in the transmitted power decreased, since the absorption coefficient k_i is larger at 200GHz than at 100GHz. By fitting the experimental curves of the measured power versus the thickness with the values of k_i, it was possible to determine the content of power in the second harmonic.

Polarization of the output EM wave was determined by reflecting it with a one-dimensional grid (wire diameter = 10μm, wire separation = 100μm) and measuring the reflected wave with a standard WR-10 horn. Maximum reflection occured when the electric field of the wave was parallel to the wire.

The frequency was measured using heterodyne systems for the frequency range around 100GHz and 200GHz. All systems had an IF in the X-band. The down conversions from the RF to the IF signals were performed using either an harmonic mixer operating at the 8th harmonic ($f_{RF} = 8f_{LO} + f_{IF}$) or a fundamental mixer. For the 200GHz frequency range, the mixer operated at the second harmonic. To avoid any ambiguity in the frequency determination, a high-pass filter (Attenuation = -60db at 100GHz) or a low-pass filter (Cut-off frequency: 165GHz [15]) was also inserted in front of the heterodyne system. Time resolved spectra were obtained by sweeping the LO frequency and looking at fixed IF frequency. Typically, it was possible to obtain a spectrum of the gyrotron over a 3GHz bandwith in 500μs. A fre-

quency spectrum without any time resolution (i.e. over the whole pulse length of 15ms) was obtained using a spectrum analyzer.

III) Experimental results

a) Fundamental frequency [9]

The time variation of the cathode voltage, mod-anode voltage, electron beam current and microwave output is shown in figure 2. The cathode voltage was set at its nominal value when the mod-anode voltage and the electron beam current I were turned on: during the start-up phase of the microwave pulse, the relativistic factor γ was constant, while the α and I varied. The time variation of these quantities was much slower than the typical linear growth time τ for the EM wave inside the resonator: τ was about 14ns at 10A, whereas the time scale for variation of α and I was of the order of 2ms.

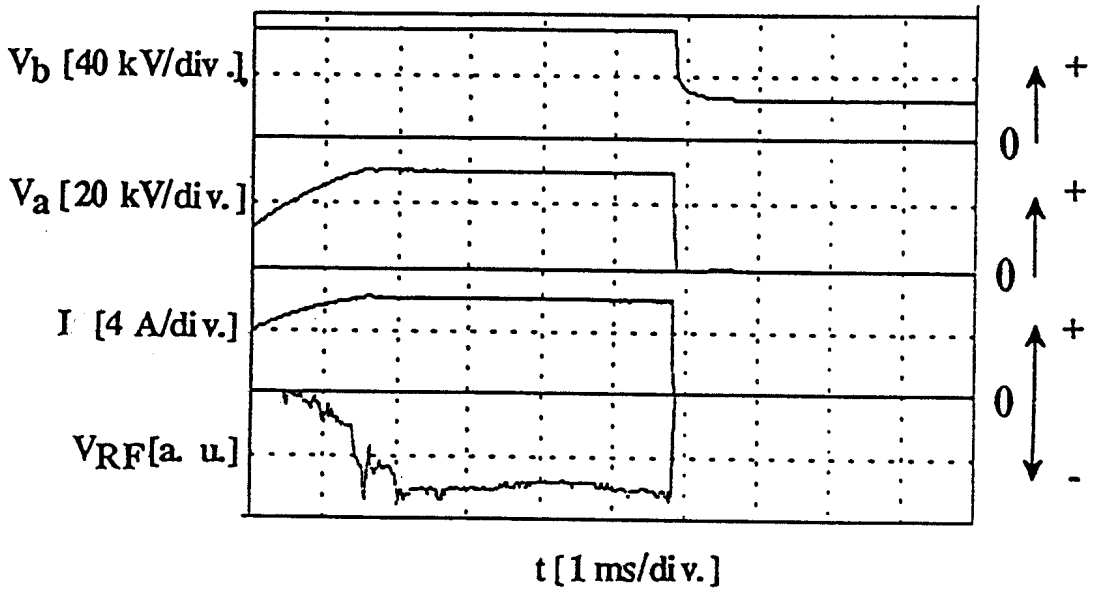

Figure 2.
Time variation of the beam voltage V_b, mod-anode voltage V_a, current I and microwave power V_{RF} from a diode

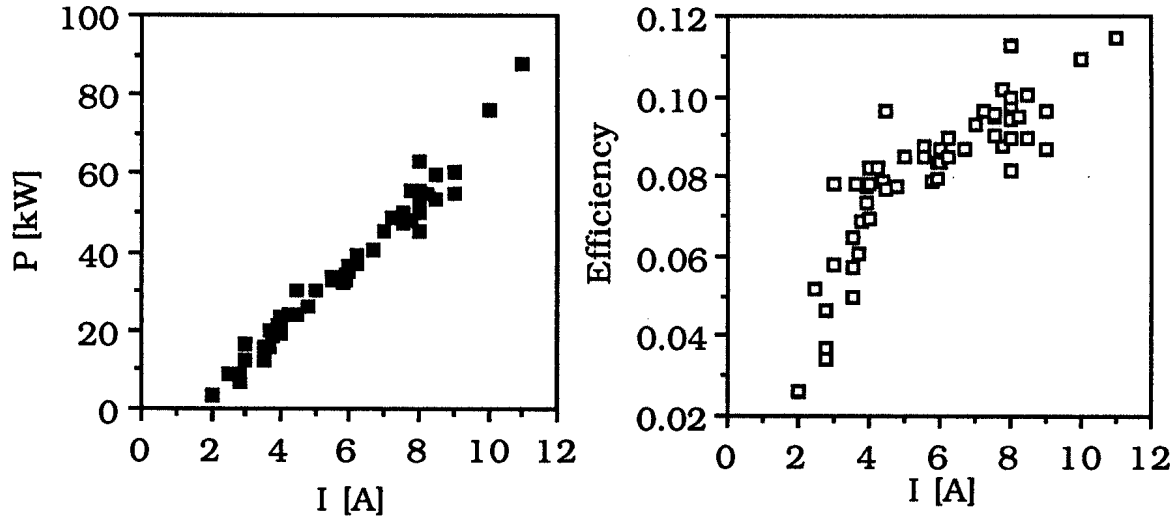

(a) (b)

Figure 3.
Variation of the power (a) and efficiency (b) with current I

The output power from the gyrotron was optimized by tuning the gun coils and the mod-anode voltage. The optimum output power and efficiency are shown on figures 3a and 3b. Note that, in the range of currents which was explored (limited by the capability of the power supply), the power and the efficiency did not saturate: the respective maxima which were reached were 90kW and 12%.

Working with a highly overmoded resonator (the operating mode is the $TEM_{0,0,227}$), an important issue was whether or not it was possible to operate in single longitudinal mode. We have found that, by proper tuning of the system, the output spectrum consisted of a single frequency: in figure 4a such a single mode spectrum is shown for an electron beam current of 9.4A. By changing parameters, the frequency spectra could exhibit two or more modes [Figs. 4b or 4c]. All the spectra were stable in time during the whole pulse. In the case of multimode, the main mode is about 6dB larger than the others. When two or more modes are excited, their frequency separation was equal to c/2d, indicating that only longitudinal modes TEM_{00q} were excited. The frequency spectrum was also shifted towards higher frequency when the current was increased: we have measured a shift of four longitudinal modes for a variation of the current I between the starting current and 10A (Fig. 5).

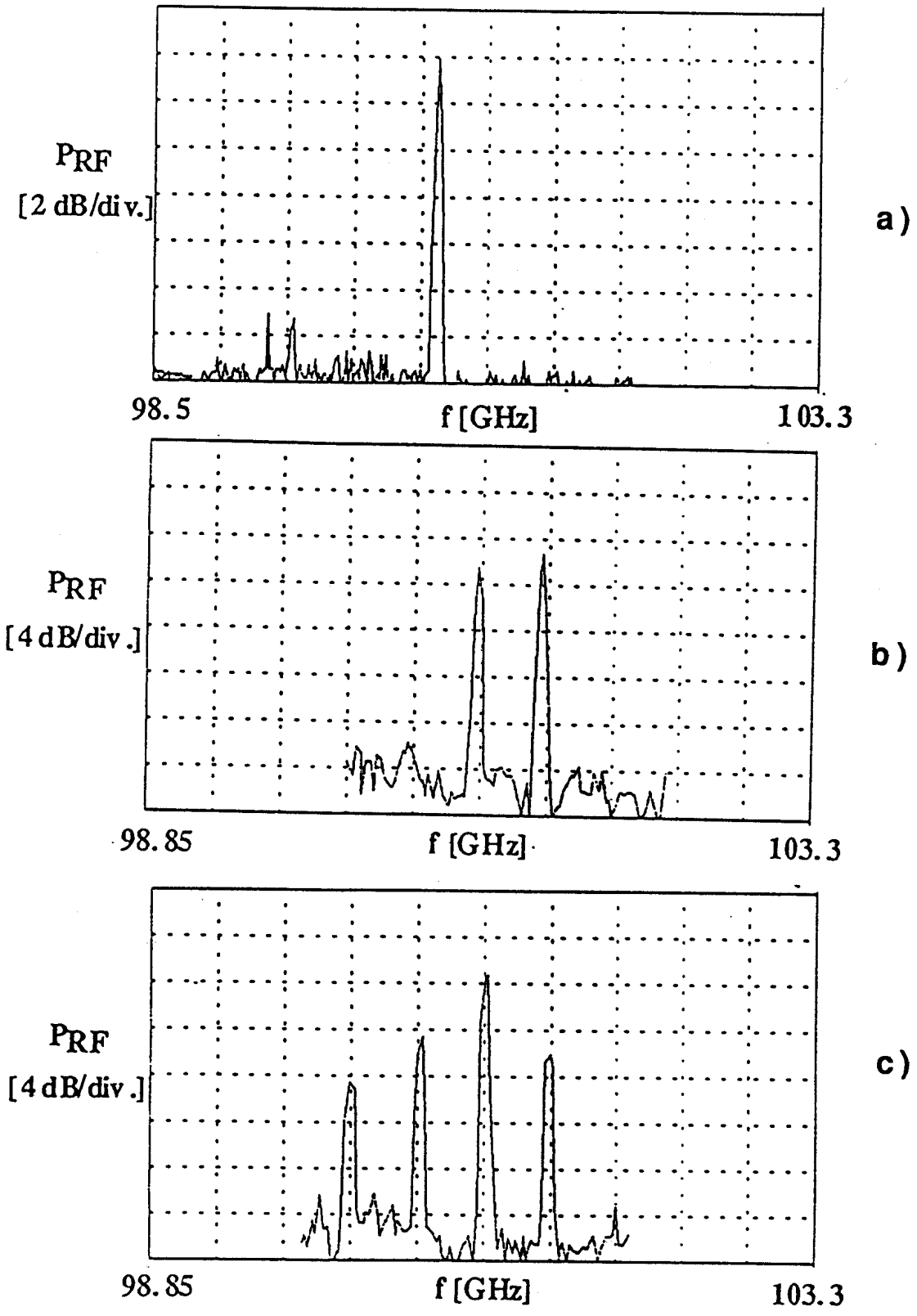

Figures 4a, b, c
Frequency spectrum

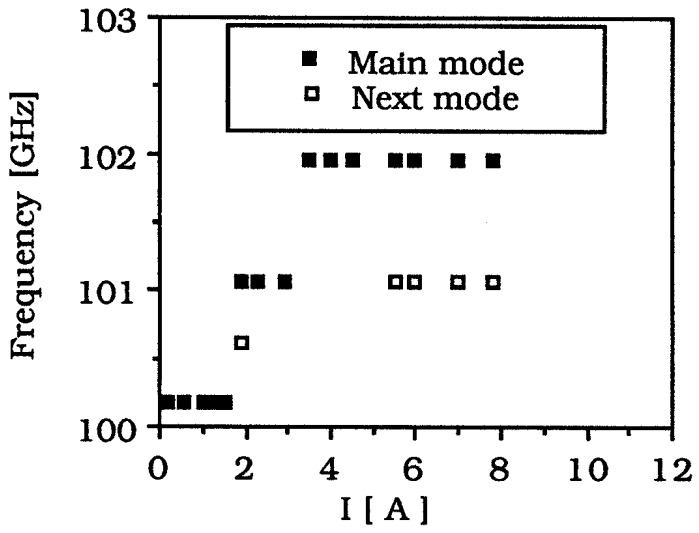

Figure 5.
Variation of the frequency versus beam current I

With the present output coupling scheme, the polarization measurement gave about 6dB difference, on average, between the cross polarizations, the dominant polarization being with the electric field perpendicular to the static magnetic field and the direction of the microwave output beam.

Another important feature of the Q.O concept is its tunability. We can distinguish between three different methods of tuning the frequency: by varying the mirror spacing d, by changing the beam voltage V_b or by changing the magnetic field B_0. All three methods have been successfully tested. By changing the mirror separation d, the frequency could be continuously tuned between two longitudinal modes with the same parity (e.g $TEM_{0,0,227}$ to $TEM_{0,0,225}$), in our case over a range of 880MHz (Fig. 6). For modes with the same parity, the averaging of the efficiency due to the standing wave pattern of the electric field gives the same result.

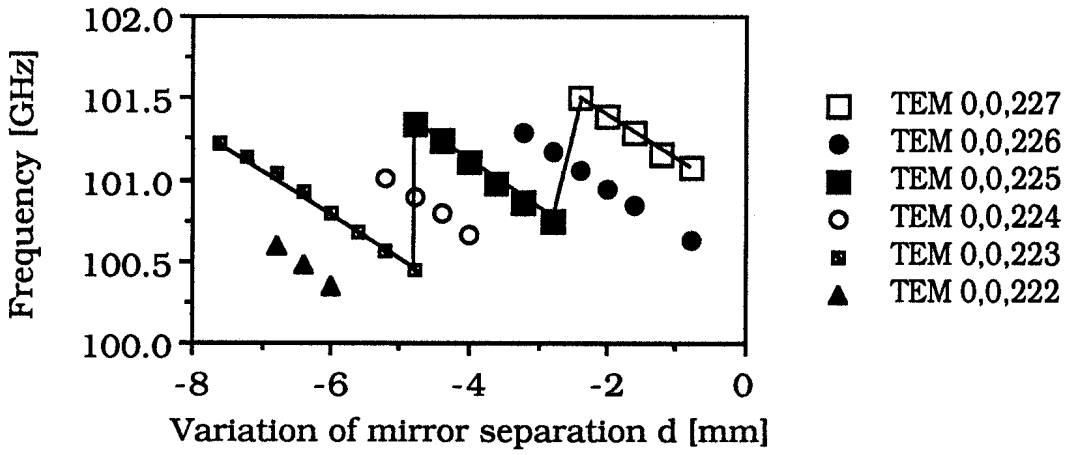

Figure 6.
Frequency variation by changing the mirror separation d

Changing the electron beam voltage can provide a method for fast frequency tuning. In our experiment the tuning range by this method was limited to about 1GHz (Fig. 7). The mode jumped by 440MHz.

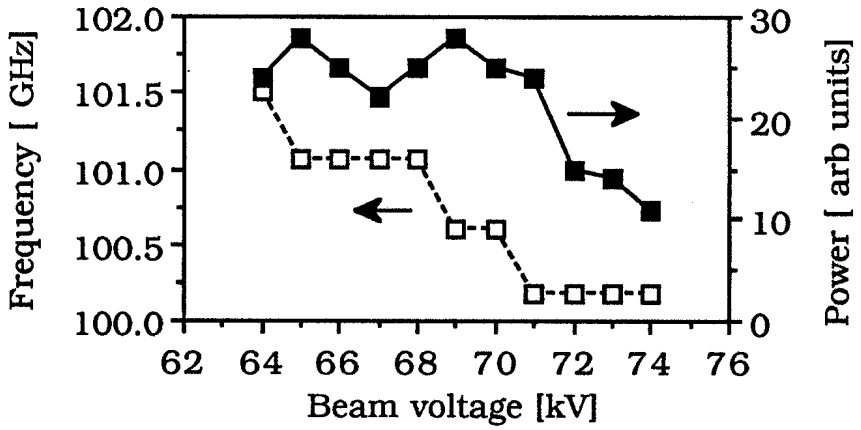

Figure 7
Variation of the frequency and power versus beam energy

Frequency tuning by changing the magnetic field B_0 allowed a larger tuning range (Fig. 8). In our experiment, the upper and lower bounds of tuning were set respectively by the superconducting magnet capabilities and by interception in the electron gun. A variation of 5% was achieved with only moderate power change.

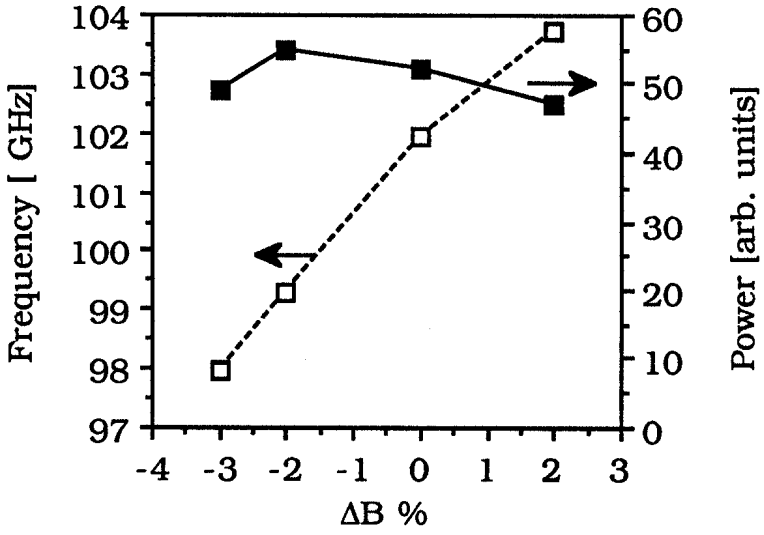

Figure 8.
Variation of the frequency and power versus magnetic field

b) Second harmonic emission [16]

Our experiments indicated that spurious second harmonic emission at 200GHz did occur, even though the resonator was designed for operation at only the fundamental. No higher harmonics were observed. Great care was taken to avoid any ambiguity in the identification of the second harmonics. Firstly, we verified that our second harmonic detection system did not give any signal when the low-pass filter was placed in front of its input. We also checked that the ratio between the signals at the second harmonic and the fundamental decreased when a Macor plate of thickness $n\lambda_{mat}/2$ was inserted in front of the respective detection systems. The power content in the second harmonic was about 20% of the one in the fundamental, using the method described above.

Simultaneous frequency measurements of the fundamental and the second harmonic were also performed. It is important to note that the emission at the second harmonic was exactly at twice the frequency of the fundamental with an accuracy of about 0.03%[16]. This second harmonic emission could also be identified as a resonator mode. We have changed the mirror separation d and observed that its frequency varied linearly with d

in a range of 1.6GHz, while the fundamental changed within 880MHz (Fig. 9).

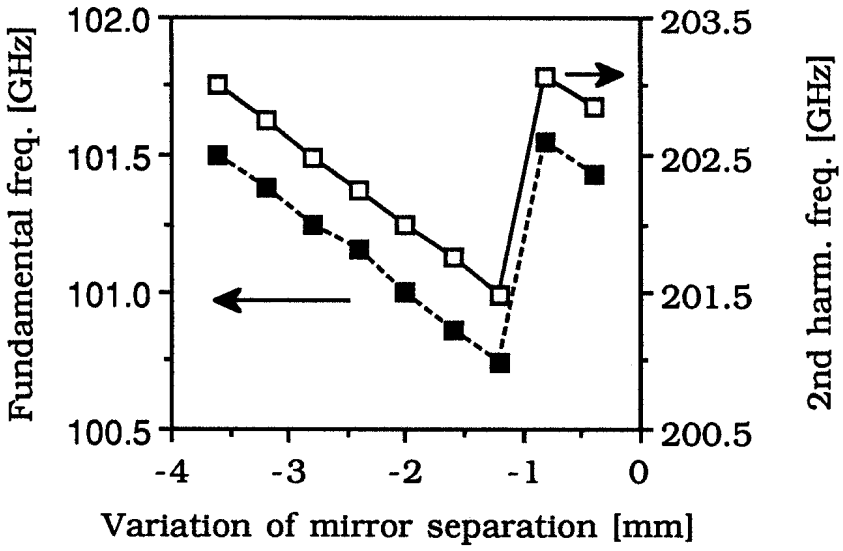

Figure 9.
Variation of the frequency of the fundamental and the second harmonic with the mirror separation d.

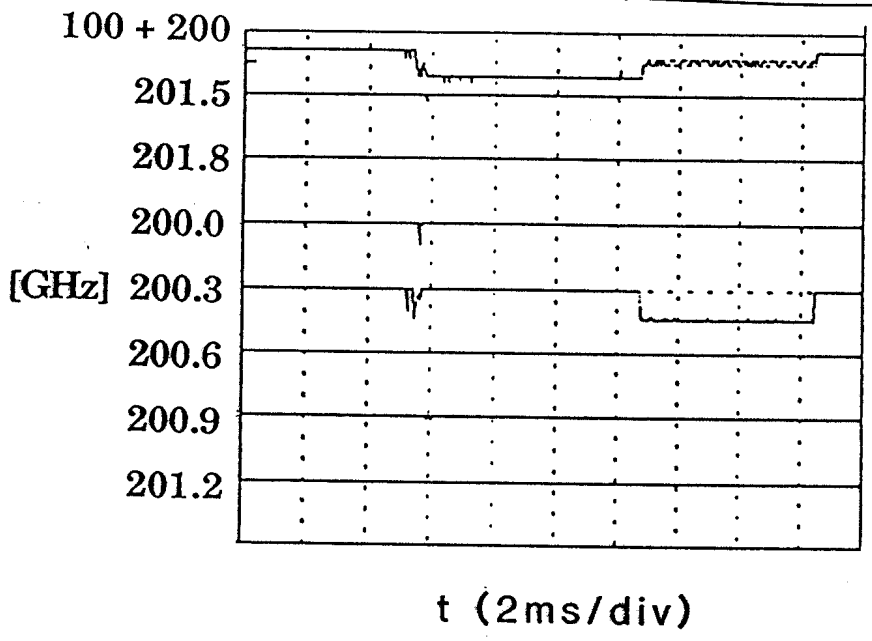

Figure 10.
Temporal variation of the total power of the spectra around 200GHz.

The presence of the second harmonic also affected the total emitted power. Figure 10 shows the time resolved signal from a diode recording the total power at the fundamental and the second harmonic and the signals at frequencies around 200GHz in band of ±150MHz. It was observed that when the second harmonic was not excited, the total efficiency was enhanced. The signal from the diode, which monitored the total power at 100 and 200GHz, dropped when the second harmonic was excited. A similar result is presented in figure 11, where the variations of the total power and the one around 200GHz are presented versus the electron beam α.

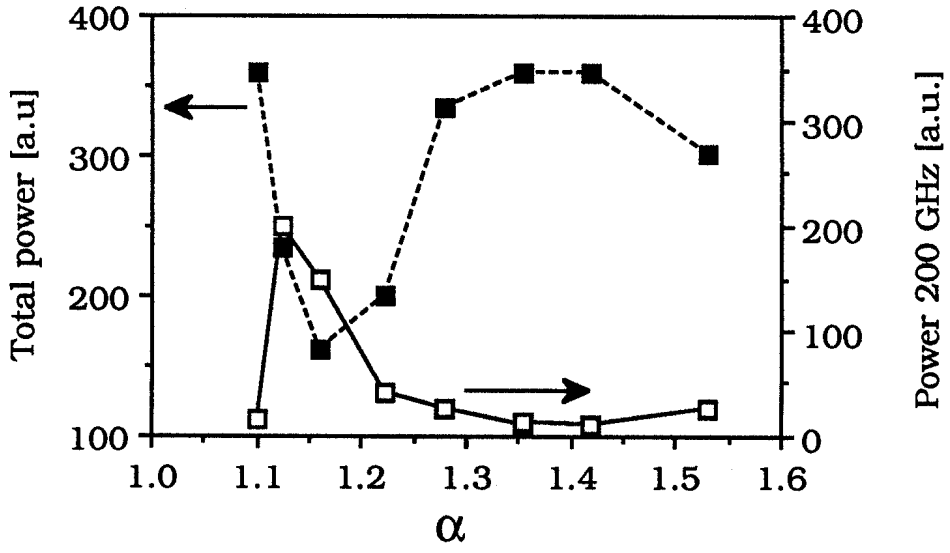

Figure 11.
Variation of the total power and the power at the second harmonic with respect to α. The two power scales are not equal due to different diode response at different frequencies

IV) Discussion

Many of the expected features of the Q.O. gyrotron have been experimentally observed. Single mode operation was obtained, confirming the theoretical predictions [3]. Different methods of frequency tuning have been demonstrated. Similar observations have been reported by Fliflet el al. [8]. In these experiments, a maximum efficiency of about 15% was obtained, a value which is comparable to ours. At higher power (up to 600kW [17]), the efficiency decreased to about 9%.

The maximum theoretical efficiency for the parameters presented in Table I is about 20% at 10A. The optimum detuning corresponds to a shift of about 4 to 5 longitudinal modes; that is, an important frequency pushing is expected if the optimum operating point is to be reached. Although experimentally such a frequency pushing was observed, its interpretation should involve the change of the electron beam voltage depression ΔV in the beam tunnel and the interaction region with the current. Based on the estimate of Fliflet et al. [8], ΔV is about 8kV at 10A. This corresponds to a decrease of the relativistic factor γ of 1.3% and to a shift of 3 to 4 longitudinal modes. We have computed the non-linear efficiency of the Q.O. gyrotron taking into account the beam depression ΔV in the interaction region. To compute the profile of the beam depression along $\underline{B}_0$, we modelize the boundary conditions in the interaction region as a conducting cylinder of a diameter equal to the mirror separation d and length l equal to the distance between the two upstream and downstream beam tunnels. At the entrance of the interaction region, ΔV is assumed to be null. $\Delta V(r,z)$ is then straight forwardly derived from the expression of the Green function for the electrostatic problem of a charge inside a conducting cylinder [18]. The DC retarding field E_z is inserted in the non-linear equations describing the electron cyclotron maser instability both in the single-mode and in the multi-mode [3] codes. The multi-mode calculations [19] indicate that the whole spectrum is shifted by about 4 modes at I above 10A compared to the case where the effect of ΔV is neglected, as shown in figure 12. The beam depression in this calculation

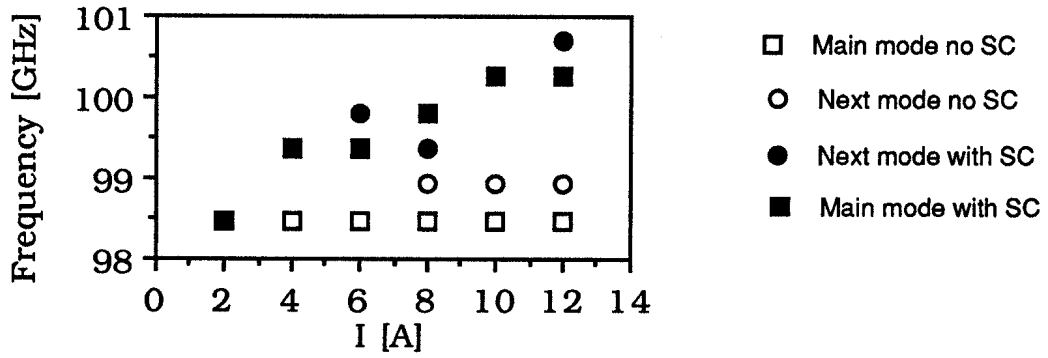

Figure 12.
Calculated frequency pushing in presence of beam depression (Plain symbols). The open symbols represent the results obtained without taking into account the beam depression.

corresponds to the actual length l in the experiment. The value of Ω/r used was not adjusted to fit the experimental conditions of figure 5. The agreement with the experimental result is fairly good. Beam depression might, therefore, account for a part of the observed frequency pushing. Further experiments are needed to clarify this important issue. Under our experimental conditions, AC space charge effects should not affect adversely the efficiency [20]. Means to control the detuning have to be implemented if the optimal detuning cannot be reached through the non-linear competition between the different unstable longitudinal modes. In a pulsed experiment, a variation in time of the beam energy could change the detuning at a given beam current, if the mode is stable [4,21]. We have verified by numerical computation that, for example, a change in the beam voltage V_b from 70 kV to 80 kV can change drastically the output power and efficiency compared to the case without voltage change. The results of such a simulation is presented in figures 13a and b. The voltage V_b is suddenly increased by 10kV (at time t=750ns in the calculation), when the system has reached an equilibrium state corresponding to V_b=70kV. The power jumps from 700kW to more than 1.2MW. The beam current I is 50A in this simulation and α is equal to 1.5. Plans to implement such scheme on our Q.O. gyrotron are under consideration. In a CW tube, magnetic field tuning is the most straightforward method to reach the optimum operating point.

The physics of the second harmonic emission is presently under investigation. The salient features which need to be understood are: 1) the frequency locking to the fundamental and 2) its influence on the efficiency. A similar phenomenon of frequency locking has been observed by Danly et al. [22]. In their experiment, no resonant cavity mode corresponded to the second harmonic. In our case, we have found that the $TEM_{0,1,454}$ mode has a resonant frequency (f=202.29GHz) which is exactly twice the one at the fundamental mode $TEM_{0,0,227}$ (f=101.14GHz). This migth explain the relatively large output power at the second harmonic compared to the results of Danly et al. [22].

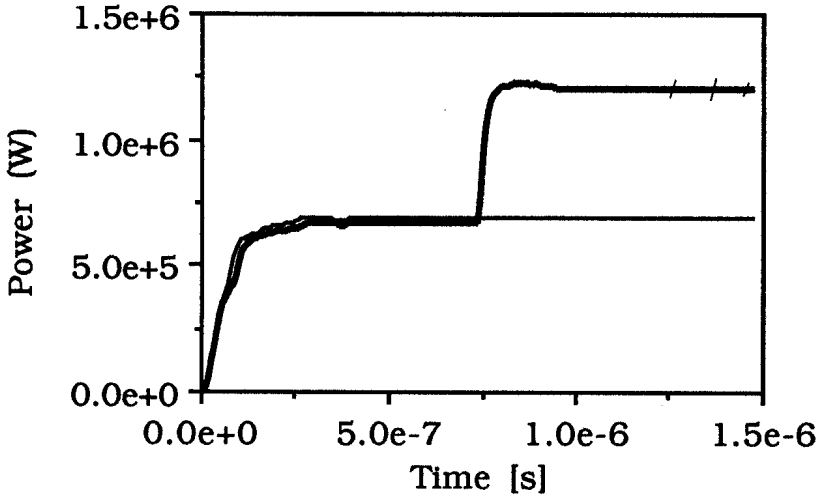

(a)

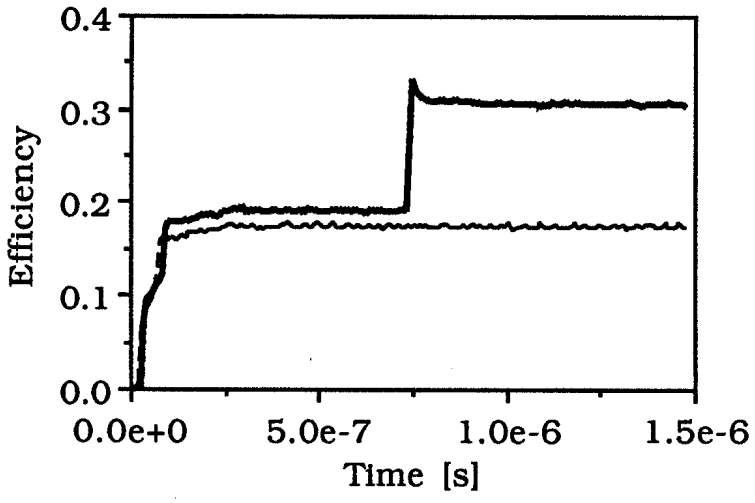

(b)

Figure 13.

Variation of the power (a) and efficiency (b) when the beam voltage V_b is increased from 70kV to 80kV (thick lines) as given by the multi-mode simulation. For comparison, we have plotted the power and efficiency for V_b = 80kV (thin lines). The beam current I is equal to 50A, α to 1.5 and the transmission T to 10%.

V) Conclusion

For electron cyclotron heating of fusion devices, it is desirable to have gyrotrons with unit power around one megawatt. Parametric studies have shown that Q.O. gyrotron at the megawatt level and at frequency higher than 100 GHz could be designed under the usual constraints on the ohmic heat load on the mirror (1.5kW/cm^2). Examples of such design are given in Table II [23]. Similar parameters were obtained by Fliflet et al. [8] in their prospectives studies of megawatt Q.O. gyrotrons.

Frequency [GHz]	150	180
Power [MW]	1	1
Beam current [A]	49	54
Beam voltage [kV]	90.2	81
α	1.6	1.7
Resonator g	-0.64	-0.9
Mirror separation d [cm]	38	42.7
Resonator transmission T [%]	8.5	10.7
Efficiency [%]	24	23

Table II - Parameters of 1MW Q.O. gyrotron.

In future development plans for Q. O. gyrotron, the following issues are of importance. Methods for increasing the efficiency have to be developed. The use of a sheet electron beam will avoid the decrease in efficiency due to the averaging over the standing wave pattern in the Fabry-Pérot resonator. Such a gun has been built and the propagation of segmented electron beam has been successfully demonstrated [24]. For future ECW systems, tens of megawatts of ECW power will be required. At present, the total system efficiency is considered to be of the order of 25%, assuming a gyrotron efficiency of 30%. Recovery of part of the spent beam energy might be beneficial. For example, a multistage depressed collector [25] could have a recovery efficiency in the 70 to 80 % range, pushing the gyrotron and system efficiency to 60% and 45% respectively.

Obtaining a gaussian output is the second issue which would require some development. The present output scheme by edge diffraction does not provide a gaussian mode. We are presently studying the implementation of a grating to couple the energy out of the resonator while maintaining the inherent gaussian profile of the radiation in the resonator. Preliminary results indicate that coupling to an HE_{11} corrugated waveguide can be achieved with high efficiency [26].

In summary, within the last two years, important steps have been made in the development of Q.O. gyrotrons. The main issues have been identified and effective solutions are under investigation.

Acknowledgements

This work was supported in part by the "Commission pour l'Encouragement de la Recherche Scientifique" under grants 1224 and 1564(1224), the "Fonds National Suisse pour la Recherche Scientifique" under grant 2000-005652, by NET under contract 330/88-1/FU-CH-NET and by internal R&D funds from the Department EKR of ABB-Infocom SA. We would like to acknowledge fruitful conversations with Drs. A. W. Fliflet, W. Kasparek and M. E. Read.

REFERENCES

[1] G. N. Rapoport et al., Radiotekh., Elektron. **12**, 633, (1967) (Radio Eng. Electron. Phys. (U.S.S.R.) **12**, 587, (1967)
F. A. Korolev et. al., Radio Eng. Electron. Phys. **15**, 1868, (1970)
A. F. Kurin et al., Izv VUZ, Radiofizika **19**, 1047, (1976)

[2] P. Sprangle et al., Phys. Rev. **A23**, 3127 (1981)
P. Sprangle et al., Appl. Phys. Lett. **38**, 310 (1981)

[3] A. Bondeson et al., Int. J. Electronics **53**, 547 (1982)
A. Bondeson et al., Millimeter and Infrared Waves **9**, K. Button ed. (Academic Press) p. 309 (1983)
A. Bondeson et al., Phys. Fluids **26**, 285 (1983)

[4] T. M. Antonsen et al., Phys. Fluids **B2**, 419 (1990)

[5] Korolev F.A. et al., Radio Eng. Electronic Physics **15**, 1868 (1970)

[6] E. C. Morse et al., J. Vacuum Sci. Technology **A3**, 1239 (1985)

[7] T. A. Hargreaves et al., Int. J. Electronics **57**, 977 (1984)
M. E. Read et al., Int. J. Electronics **65**, 309 (1988)

[8] A. W. Fliflet et al., Phys. Rev. Lett. **62**, 2664 (1989)
A. W. Fliflet et al., Phys. Fluids **B2**,1046 (1990)
A.W. Fliflet et al., IEEE Trans. Plasma Science **18**, 306 (1990)
A. W. Fliflet et al., J. Fusion Engineering **9**, 31 (1990)

[9] J. Ph. Hogge et al., Conf. Digest 14th Int. Conf. on Infrared and Millimeter Waves, Würzburg, F.R.G., 1989, SPIE **1240** , 233 (1989)
S. Alberti et al., Phys. Fluids **B2**, 1654 (1990)

[10] A. Perrenoud et al., Int. J. Electronics **57**, 985 (1984)

[11] H. Stickel, Int. J. Electronics **64**, 63 (1988)

[12] M. N. Afsar et al., IEEE Trans. Instrumentation and Measurements **IM-25**, 290 (1976)

[13] J.L. Byerly et al., Int. J. Electronics **57**, 1033 (1984)

[14] M. N. Afsar, IEEE Trans. Instrumentation and Measurements **IM-36**, 530 (1987)
M. N. Afsar et al., Int. J. IR and MM Waves **3**, 319 (1982)

[15] B. W. Davis et al., Int. J. IR and MM Waves **6**, 3 (1985)

[16] S. Alberti et al., Conf. Digest 14th Int. Conf. on Infrared and Millimeter Waves, Würzburg, F.R.G., 1989, SPIE **1240** , 231 (1989)
S. Alberti et al., Lausanne Report LRP 402/90 (April 1990), to be published in Phys. Fluids **B2**, November (1990)

[17] A. W. Fliflet, Private Communication (1990)

[18] See for example "Classical Electrodynamics", J.D. Jackson, [John Wiley and Sons], p. 134 (1975)

[19] S. Alberti et al. , to be published

[20] R. G. Kleva et al., Phys. Fluids **31**, 375 (1988)

[21] B. Levush et al., IEEE Trans. Plasma Sci. **18**, 260 (1990)

[22] B. G. Danly et al., Appl. Phys. Lett. **46**, 728 (1985)

[23] T. M. Tran et al., IEEE Trans. Electron Dev. **ED 36**, 1983 (1989)

[24] M. E. Read et al., Conf. Digest 13th Int. Conf. on Infrared and Millimeter Waves, 1988, SPIE **1039**, 279 (1988)
M. E. Read et al., Conf. Digest 14th Int. Conf. on Infrared and Millimeter Waves, Würzburg, F.R.G., 1989, SPIE **1240**, 79 (1989)
M. E. Read et al., to be published

[25] A. Sh. Fix et al., Int. J. Electronics **57**, 821 (1984)
M. E. Read et al., Conf. Digest 13th Int. Conf. on Infrared and Millimeter Waves, Honolulu, USA., 1988, SPIE **1039**, 181 (1988)
M. Q. Tran et al., Conf. Digest 14th Int. Conf. on Infrared and Millimeter Waves, Würzburg, F.R.G., 1989, SPIE **1240**, 318 (1989)
T.V. Borodachyova et al., in "Gyrotron", V.A. Flyagin ed. ,p. 161 (1989)
M.E. Read et al., MTTT Trans. Electron. Devices, **ED37**, 1579 (1990)

[26] J. Ph. Hogge et al., Conf. Digest 15th Int. Conf. on Infrared and Millimeter Waves, Orlando, USA., December1990